ISBN: 978-3-95450-208-0 doi:10.18429/JACoW-IPAC2019-TUPRB074

START-TO-END SIMULATIONS OF THE COMPACT LIGHT PROJECT BASED ON AN S-BAND INJECTOR AND AN X-BAND LINAC*

E. Marin†, R. Muñoz Horta, F. Perez,
ALBA Synchrotron, 08290 Cerdanyola del Valles, Spain
A. Aksoy, Ankara University Institute of Accelerator Technologies, UA-IAT, Ankara, Turkey
S. Di Mitri, Elettra Sincrotrone Trieste, 34149 Basovizza, Italy
A. Latina, CERN, 1211 Geneva 23, Switzerland
S.B. van der Geer, Pulsar Physics (PP), The Netherlands.

Abstract

In this paper we report the start-to-end simulation results of one of the options under consideration for the Compact-Light Project (XLS). The XLS is a hard X-ray Free Electron Laser under design, using the latest concepts for bright electron photo injectors, very high-gradient X-band structures, and innovative short-period undulators. Presently there exist various tracking codes to conduct the design process. Therefore identifying the most convenient code is of notable importance. This paper compares the tracking codes, Placet and General Particle Tracer, using the XLS lattice based on a *S* and *X*-band Injector. The calculation results in terms of beam quality and tracking performance of a full 6-D simulation are presented.

INTRODUCTION

CompactLight [1] is a consortium funded by the European Union that encompasses 24 different institutions from around the world [2]. The latest generation of light sources, the Free Electron Lasers (FELs) [3], are capable of delivering high-intensity photon beams of unprecedented brilliance and quality, providing large potential for science. Examples of operating FELs in the European Union are the FERMI [4] and FLASH [5] facilities delivering soft X-rays and more recently the SwissFEL [6] and the EuroXFEL [7] producing hard X-rays.

Relevant advances in several fields that drive the design process of an FEL have been made over the past years. To mention a few:

- Lower emittance and higher repetition rate photo-injectors.
- High-gradient linacs – Gradients in excess of 100 MV/m, based on CLIC Technology [8].
- Advanced concept undulators.
- Better beam dynamics codes and optimization tools.

These developments could significantly reduce the cost and size of such a facility, making this option a more affordable investment.

* This project has received funding from the European Union's Horizon2020 research and innovation programme under grant agreement No 777431.
† emarin@cells.es

This paper focuses its attention on the beam dynamics code item just presented. Identifying the most convenient code for conducting a comprehensive and optimized study is of notable importance.

TRACKING CODES

The tracking codes selected for comparison are Placet [9] and General Particle Tracer (GPT) [10]. These codes are chosen because of their different implementation of the physics that rule the beam dynamics of particles under the influence of electro-magnetic fields. Placet is often called a kick-code, meaning that all beamline elements have an associated map that transports the particle through that given element. Thus individual particles are tracked by consecutively applying the transport maps through the beamline. In contrast, GPT solves the equation of motion of individual particles by constructing ordinary differential equations (ODE), and solving them, using a 5^{th}-order embedded Runge-Kutta integrator [11] with adaptive step-size. Both codes describe the 6-D phase space of the beam, however Placet uses position $(x,\ y,\ z)$, angles $(x',\ y')$ and energy (E) as a function of the nominal longitudinal coordinate (s), whereas GPT describes the position $(x,\ y,\ z)$ and momentum $(p_x,\ p_y,\ p_z)$, as a function of time. Indeed, the ODEs are solved for a given time step defined by the user, the size of which drives the accuracy of the calculations at the expenses of CPU time.

In our code comparison study we use the XLS design (version 2016) obtained by Placet. The lattice is converted into GPT lattice syntax and the tracking is then repeated. In the following, we first describe the considered lattice and the initial beam distribution. Secondly the lattice conversion from Placet to GPT is explained. Afterwards the simulations results are compared as well as the CPU performance. Finally the examination of the results and the on-going work concludes the paper.

XLS LATTICE

The XLS lattice can be divided into 3 different sections, namely Injector, Linac and Undulator. An initial list of design parameters is given in [1] but subject to modifications due to future user requirements.

In this study only the Linac section is considered for simulations which considerably reduces the computing time, since space-charge effects are neglected, as the beam is al-

ISBN: 978-3-95450-208-0 doi:10.18429/JACoW-IPAC2019-TUPRB074

ready relativistic. Therefore the initial beam distribution provided by the Injector is obtained by the working group responsible of its design. The following sub-section provides the details of the injected beam into the Linac.

The Linac is responsible of increasing the beam energy and also reducing the bunch length while preserving the beam quality to its best, for an optimal hard X-ray photon beam generation, in the Undulator section. Figure 1 shows an schematic layout of the considered XLS option.

Table 2 shows the most relevant beam parameters at the entrance and the exit of the Linac section considered in this study.

Table 1: Beam Parameters at the Entrance and Exit of the XLS Linac

Parameter	Unit	Entrance	Exit
Energy	[GeV]	0.129	6.2
Bunch length (rms)	[μm]	804	10
Norm. energy spread (rms)	[%]	0.12	0.2
Norm. trans. emmittance	[μm]	0.2	0.3

Injector

The working group in charge of designing the XLS Injector is currently considering S-band and C-band technologies as possible candidates to generate the electron beam. In our case we consider the S-band option capable of generating a beam that satisfies the parameters presented in Table 2. Figure 2 shows the phase space of the electron beam at the exit of the Injector.

Linac

The linac is split in 3 sub-linacs, namely L1, L2 and L3 which are separated by the bunch compressors (BC1 and BC2) as shown in Fig. 1. L1 increases the beam energy up to 298 MeV by means of S-band cavities running at 32 deg off-crest in order to introduce the longitudinal chirp required for bunch compression. The linearization is accomplished by the X-band linearizer running at 273 deg, located upstream BC1. The first bunch compressor reduces the bunch length from $\approx 800\mu$m down to 85 μm thanks to a 4-dipole chicane. Further downstream, the linacs L2 and L3 consist of X-band modules [12] that increase the beam energy up to 2.2 GeV and 6.2 GeV, respectively. Each module is composed of several X-band cavities designed for an optimal gradient of 65 MV/m. L2 cavities run at a phase of 22 deg off-crest in order to preserve the longitudinal chirp required at BC2 for further compression, while cavities at L3 run at a phase of –4 deg off-crest, in order to almost exploit the full capacity of the accelerating gradient. BC2 reduces the bunch length from 85 μm to $\approx 10\mu$m.

SIMULATIONS

The considered lattice was originally designed in 2016 in Placet and complies with the specifications shown in Table 2 using the beam distribution presented in the previous section as initial beam. The lattice is mainly composed of rectangular bending magnets, quadrupoles and accelerating cavities. These elements are directly converted with the built-in elements in GPT. However there are 3 considerations that need special attention when converting the lattice from Placet to GPT:

1. Coordinate system.
2. Input power and phases of the travelling wave cavities.
3. Fringe field effects.

The first item is due to the inherently different way of treating the reference system of coordinates. GPT features the peculiarity that only the built-in elements, *sectormagnet* and *ccsflip*, can change the coordinate system. This requires the definition of custom coordinate systems for every bending magnet in the beamline. Also in the conversion process the user needs to keep track of the center of the elements with respect to the center of the last bending magnet. The second item is related to the fact that GPT is a time-domain tracking code. Therefore all dynamic elements, such as travelling wave cavities, require adjustments of their phases and input power variables, in order to set them at the corresponding values of phase and gradient given by design. This has no implications to static elements, such as dipoles and quadrupoles. However the mentioned static elements feature fringe fields that are represented differently in the codes. Therefore a re-matching of the first 3 quadrupole magnets at each side of the BCs is required, in order to properly match the Twiss parameters between the linac sections and the BCs.

Regarding collective effects, the wake-fields present in the *S* and *X*-band cavities are included in Placet as well as GPT.

Although the effect of coherent synchrotron radiation can be included in simulations for both codes, yet it is not considered in our study.

Results

Figure 3 shows the evolution of the transverse beam sizes ($\sigma_{x,y}$) along the XLS obtained by Placet and GPT. Differences in both planes occur already at L1, suggesting that the fringe field of the accelerating cavities and quadrupoles are affecting the beam differently. Also, after the BCs the beam sizes obtained by GPT show a miss-match that is attenuated along L2 and L3. Again this could be explained by the fringe fields of the bending magnets which are described significantly different in both codes.

Figure 4 shows the propagation of the bunch length (σ_z) and normalized energy spread ($\Delta p/p$) along the XLS obtained by Placet and GPT. With regards of the longitudinal plane, a good agreement is observed for the bunch length, but the normalized energy spread along the entire XLS, presents deviations. The observed ripple on the solid blue curve around the 50 m location (after BC1), could be due to a small difference in phase settings of the L2 cavities which

ISBN: 978-3-95450-208-0 doi:10.18429/JACoW-IPAC2019-TUPRB074

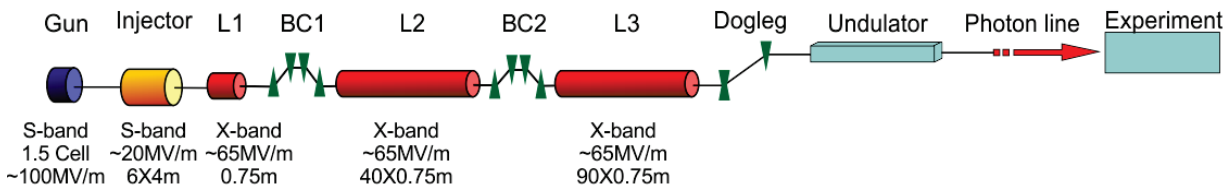

Figure 1: Schematic layout of the XLS 2.A option version 2016.

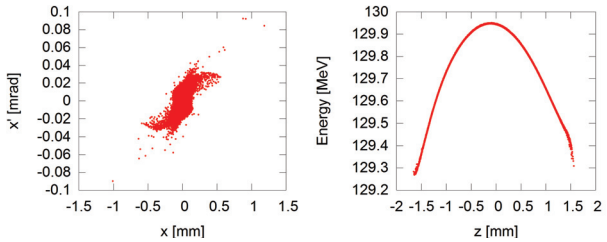

Figure 2: Horizontal (left) and longitudinal (right) phase space obtained at the exit of the S-band Injector.

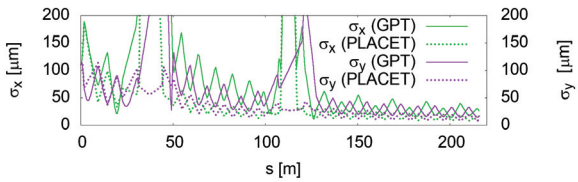

Figure 3: Horizontal (purple) and vertical (green) beam sizes along the XLS evaluated by Placet (dash) and GPT (solid).

might be cured by re-optimizing the phases in GPT. Also the final values of $\Delta p/p$ differ by $\approx$ 20 %, which also suggest that the setting of phases is not correctly done in the GPT lattice.

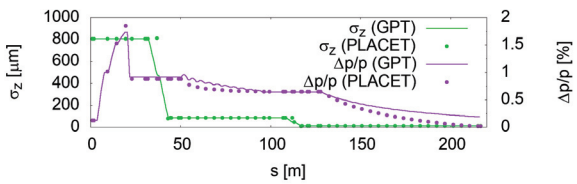

Figure 4: Evolution of σ_z and $\Delta p/p$ along the XLS evaluated by Placet (dash) and GPT (solid).

Table 2: Beam Properties at the End of L3 Obtained by Placet and GPT

Parameter	Unit	Placet	GPT
Energy	[GeV]	6.2	6.2
Bunch length (rms)	[μm]	10.1	10.2
Norm. energy spread (rms)	[%]	0.17	0.19
Norm. trans. emmittance	[μm]	0.22	0.27

Tracking Performance

Accuracy (*acc*) and number of particles (N) are the relevant variables to compare the CPU-tracking performance of the codes. In Placet the user can improve the accuracy of the simulations as $\propto \sqrt{N}$ by increasing the number of particles, leading to an increase of CPU time $\propto N$. In GPT the accuracy of the calculations can be set by the *accuracy*-command. Doing so the time-step used to solve the ODE is adapted accordingly to satisfy the required *acc* by the user, allowing to reduce N, thus the CPU time, while preserving the required *acc*. Figure 5 shows the percentage error of $\Delta p/p$ with respect to the *acc* value (N is fixed at 10^4) and also the percentage error of σ_z (*acc* = 4) with respect to N. Increasing N beyond 10^4 improves the *acc* $\leq$ 0.1 % while

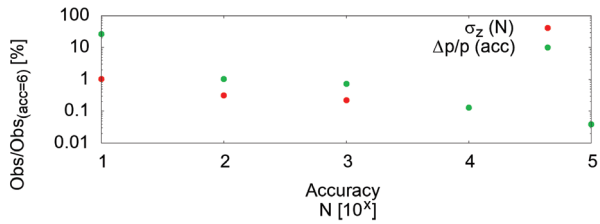

Figure 5: Deviation of σ_z and $\Delta p/p$ vs. *acc* and N.

the computing time increase dramatically, going from 21 s to 27 min. Similarly, increasing the *acc* $\geq$ 5 decreases the percentage error by $<$ 0.05 %. The obtained CPU time of tracking 10^5 particles along the considered XLS takes 6 s in Placet while GPT needs 663 s at an *acc* = 4. However only 10^4 particles are required by GPT to obtain an error in the results $<$ 0.1%, similar to Placet, which reduces the CPU time to 21 s.

CONCLUSIONS

A reasonable agreement ($\approx$ 20 %) has been found between the tracking codes Placet and GPT in terms of the most relevant observables, despite the different nature of the codes. This difference is suspected to be a consequence of the fringe fields but further investigation is required. In terms of computing time Placet is a factor 3 times faster than GPT at a similar level of accuracy, which makes it more attractive to conduct consuming time calculations as lattice design and imperfection studies. Nevertheless GPT can load external field-maps (e.g. travelling wave cavities), which could be of interest to determine the robustness of the lattice at a later stage of the design.

ISBN: 978-3-95450-208-0 doi:10.18429/JACoW-IPAC2019-TUPRB074

REFERENCES

[1] G. D'Auria and J. A. Clarke, "The CompactLight Design Study Project", presented at the 10th Int. Particle Accelerator Conf. (IPAC'19), Melbourne, Australia, May 2019, paper TUPRB032, this conference.

[2] "CompactLight Project Homepage.", http://www.compactlight.eu.

[3] C. Pellegrini, "X-ray free-electron lasers: from dreams to reality.", *Physica Scripta, T169*, Dec. 2006.

[4] Bocchetta, C.J. *et al.*, "FERMI@Elettra FEL Conceptual Design Report", *ST/F-TN-07/12*, 2007, https://www.elettra.eu

[5] B. Faatz, J. Feldhaus, K. Honkavaara, J. Roßbach, S. Schreiber, and R. Treusch, "FLASH Status and Upgrade", in *Proc. 31st Int. Free Electron Laser Conf. (FEL'09)*, Liverpool, UK, Aug. 2009, paper WEOA02, pp. 459–462.

[6] H.-H. Braun, "SwissFEL, the X-ray Free Electron Laser at PSI", in *Proc. 34th Int. Free Electron Laser Conf. (FEL'12)*, Nara, Japan, Aug. 2012, paper MOOB04, pp. 9–12.

[7] M. Altarelli *et al.*, "XFEL: The European X-Ray Free-Electron Laser. Technical design report", *10.3204/DESY_06-097*, 2006.

[8] T. Argyropoulos *et al.*, "Design, fabrication, and high-gradient testing of an *X*-band, traveling-wave accelerating structure milled from copper halves", *Phys. Rev. Accel. Beams*, vol 21, p. 061001, June 2018. 10.1103/PhysRevAccelBeams.21.061001.

[9] A. Latina, Y. I. Levinsen, D. Schulte, and J. Snuverink, "Evolution of the Tracking Code PLACET", in *Proc. 4th Int. Particle Accelerator Conf. (IPAC'13)*, Shanghai, China, May 2013, paper MOPWO053, pp. 1014–1016.

[10] S.B. van der Geer and M.J. de Loos (2004) "GPT (General-Particle Tracer)", http://www.pulsar.nl/gpt.

[11] William H. Press, Brian P. Flannery, Saul A. Teukolsky and William T. Vetterling, "The Art of Scientific Computing", *Numerical Recipes*, Cambridge University Press, 2nd edition, 1992.

[12] A. Latina *et al.*, "CompactLight Design Study", in *Proc. 60th ICFA Advanced Beam Dynamics Workshop on Future Light Sources (FLS'18)*, Shanghai, China, Mar. 2018, pp. 85–88. doi:10.18429/JACoW-FLS2018-WEP1WC02